1·5 μm grating wavelength-demultiplexer on InP-based waveguide', *Electron. Lett.*, 1989, **25**, (21), pp. 1441–1442
4 SOOLE, J. B. D., SCHERER, A., LEBLANC, H. P., ANDREADAKIS, N. C., BHAT, R., and KOZA, P. A.: 'Monolithic InP-based grating spectrometer for wavelength division multiplexed systems at 1·5 μm', *Electron. Lett.*, 1991, **27**, pp. 32–134
5 CREMER, C., EMEIS, N., SCHIER, M., HEISE, G., EBBINGHAUS, G., and STOLL, L.: 'Grating spectrograph integrated with photodiode array in InGaAsP/InGaAs/InP', *Photonics Technol. Lett.*, 1992, **4**, pp. 108–110

OPTICAL-GAIN ENHANCEMENT IN RESONANT-CAVITY HETEROJUNCTION BIPOLAR PHOTOTRANSISTOR THROUGH EMITTER-EDGE THINNING

F. Y. Huang, G. L. Zhou, Z. F. Fan, G. B. Gao, A. E. Botchkarev, B. Sverdlov and H. Morkoç

Indexing terms: Optical receivers, Phototransistors, Bipolar devices

The authors use a lateral emitter resistor in floating base GaAs/InGaAs/AlGaAs heterojunction bipolar phototransistors to reduce the surface recombination in the vertical wall of the emitter–base junction and increase the photosensitivity at low injection levels. The same process also reduces the dark current in the reverse biased collector junction.

Owing to their potential applications as photoreceivers with high-speed and wavelength-selective capabilities [1, 2], there has recently been a great deal of development in resonant-cavity enhanced heterojunction bipolar phototransistors (RCE-HPTs). For practical applications of the RCE-HPTs in optical communications and optical logic, it is axiomatic that small reverse-bias leakage currents and large optical gains for low-level photodetection are desirable.

Recently emitter-edge thinning in GaAs/AlGaAs double heterostructure bipolar transistors (HBTs) has been used to improve their emitter–base forward bias characteristics [3, 4]. In this Letter, we exploit the emitter-edge thinning to enhance the optical gain and reduce the reverse-bias leakage current in a GaAs/InGaAs/AlGaAs RCE-HPT.

The RCE-HPT consists of a bottom mirror with 13 pairs of quarter-wave stacks with a maximum reflectivity of about 90% at the central wavelength of 900 nm. The top mirror is formed by the semiconductor/air interface. This gives a reflectivity of about 30%. The absorber layer consists of 0·1 μm $In_{0.05}Ga_{0.95}As$ on the top of the collector. The composition of the layers is chosen such that light is only absorbed by this thin InGaAs layer around the central wavelength. The total thickness of the cavity is adjusted properly to satisfy the phase matching conditions giving a maximum quantum efficiency of 43% with an active layer thickness of 0·1 μm [5].

The layer structure along with the cross-sectional view of the device configuration is presented in Fig. 1. The epitaxial layers were grown by molecular beam epitaxy (MBE) on an n^+-GaAs substrate. The growth was initiated with a 0·5 μm n^+-GaAs buffer layer. A 13-period AlAs/GaAs quarter-wave stack serves as a high reflectivity mirror. A 527 nm n^+-GaAs ($n = 4 \times 10^{18}\,cm^{-3}$) was layer grown on the top of the mirror as the subcollector. The active layer of i-$In_{0.05}Ga_{0.95}As$ of thickness 100 nm is sandwiched between the n^+-GaAs collector ($n = 5 \times 10^{16}\,cm^{-3}$) of thickness 527 nm and the i-GaAs spacer layer of thickness 10 nm. What follows is a 100 nm p^+-GaAs ($p = 5 \times 10^{18}\,cm^{-3}$) base and a 10 nm i-GaAs spacer. An n^+-$Al_{0.3}Ga_{0.7}As$ ($n = 2 \times 10^{18}\,cm^{-3}$) of thickness 198 nm was then grown as the emitter. A 50 nm n^+-GaAs ($n = 5 \times 10^{18}\,cm^{-3}$) was finally grown as a cap layer.

Floating base RCE-HPT devices were fabricated by standard photolithography and wet chemical etching. Square mesas ($150 \times 150\,\mu m^2$) were etched down to the GaAs subcollector layer. Ti/Au was then evaporated to form contacts to

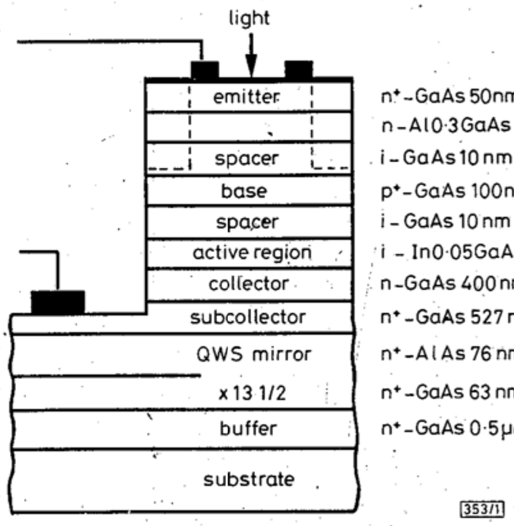

Fig. 1 *Schematic layer structure and cross-sectional view of the RCE-HPT*

both the emitter and collector. The topography was such that the incident light could pass through a square window ($50 \times 50\,\mu m^2$) interior to the emitter contact, as illustrated in Fig. 1. For emitter thinning, the fabricated devices were covered by a filtered photoresist (PR) and the emitter region exterior to the emitter contact metal was progressively etched in an $NH_4OH : H_2O_2 : H_2O$ (3 : 1 : 300) solution with an etching rate of about 20 Å/s. The lateral resistor of the emitter-edge, depicted as the areas enclosed by the dashed lines in Fig. 1, was removed by wet etching.

The photoresponse of the RCE-HPT was measured using a tungsten lamp as the light source. After passing through a monochromator, the light beam was focused onto the device. The photocurrent signal was then sensed by a lock-in amplifier. The photocurrent response spectrum of the RCE-HPT is shown in Fig. 2. The resonant cavity effect is evidenced by the

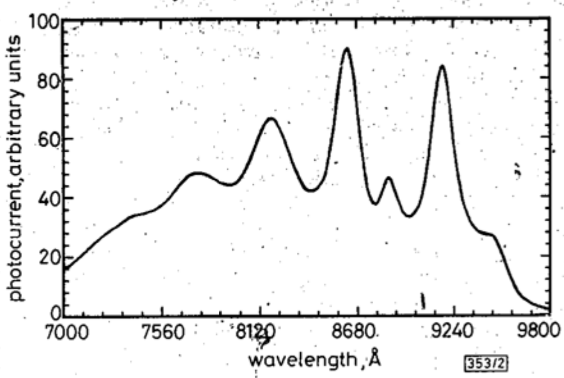

Fig. 2 *Photoresponse of resonant-cavity enhanced heterojunction bipolar phototransistor*

presence of resonance peaks around the expected wavelengths in the spectrum. The main resonance peak deviates slightly from the designed value, which may be due to a small deviation in the thickness of the optical cavity as compared to the design.

Enhancement of optical gain due to the reduction of surface recombination by surface recessing is presented in Fig. 3. When etching the lateral resistor of the emitter region, the revese biased leakage current of a single device was measured progressively for each etching step. The photosensitivity at the peak resonance wavelength was then measured for the same device. The enhancement factor as represented by the ratio of collector current (I), in a device exhibiting the smallest leakage current by surface recessing, to that without surface recessing

(I_0) is shown as a function of the incident optical power through the emitter window. As shown in Fig. 3, when the optical power is high the collector currents for both cases are

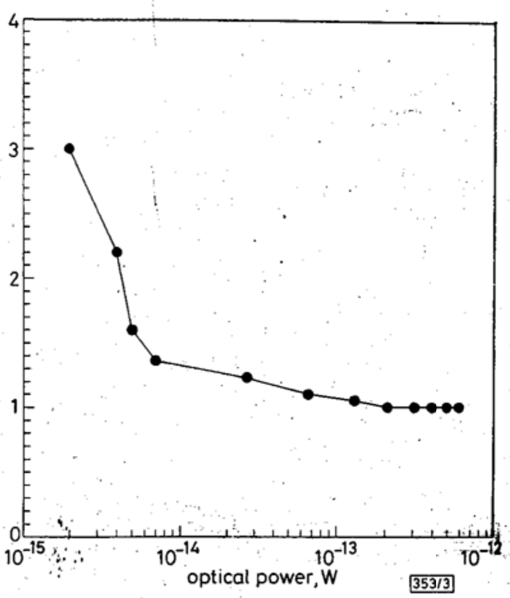

Fig. 3 *Enhancement of collector current by surface recessing as function of incident optical power*

Under high level light input, the ratio of the collector current with surface recessing (I) to that without surface recessing (I_0) (enhancement factor) is close to 1. As the incident optical power decreases, the ratio increases with a maximum enhancement factor of ~3 with the lowest light power detected with our measurement apparatus. The collector current at the largest incident optical power is ~300 pA

nearly the same. This implies that the surface recombination component is negligible for large photocurrent signals. As we reduce the optical power, photocurrent becomes smaller and the surface recombination becomes significant. As seen from Fig. 3, a maximum enhancement of about a factor of three has been achieved for the lowest optical power detected with our measurement apparatus.

In conclusion, we have fabricated a resonant-cavity enhanced heterostructure bipolar phototransistor with enhanced optical gain at low level illumination by a proper surface recessing of the lateral emitter region. The same process applied to the vertical walls of the base–collector junction also results in reduced leakage current in the collector junction and hence low dark current. The reduction of dark current and enhancement in the optical gain are important for low level photodetection.

Acknowledgment: This work has been supported by the Office of Naval Research (ONR) through grant No. N00014-88-K-0724. H. Morkoç acknowledges support of Department of Energy through grant No. DEFGO2-91EK45439.

16th March 1993

F. Y. Huang,* G. L. Zhou, Z. F. Fan, G. B. Gao, A. E. Botchkarev, B. Sverdlov and H. Morkoç (*Material Research Laboratory and Coordinated Science Laboratory, University of Illinois at Urbana-Champaign, 104 South Goodwin Avenue, Urbana, IL 61801, USA*)

* Also with the Department of Material Science and Engineering

References

1 ÜNLÜ, M. S., KISHINO, K., CHYI, J.-I., ARSENAULT, L., REED, J., MOHAMMAD, S. N., and MORKOÇ, H.: 'Resonant cavity enhanced AlGaAs/GaAs heterojunction phototransistors with an intermediate InGaAs region in the collector', *Appl. Phys. Lett.*, 1990, **57**, pp. 750–752

2 DODABALAPUR, A., and CHANG, T. Y.: 'Resonant-cavity InGaAlAs/InGaAs/InAlAs phototransistors with high gain for 1·3–1·6 μm', *Appl. Phys. Lett.*, 1992, **60**, pp. 929–931

3 LIU, W. C., GUO, D. F., and LOUR, W. S.: 'Application of an emitter edge-thinning technique to GaAs/AlGaAs double heterostructure-emitter bipolar transistors', *Appl. Phys. Lett.*, 1992, **61**, pp. 1441–1443

4 GAO, G. B., FAN, Z. F., TERAGUCHI, N., SHEN, T. C., and MORKOÇ, H.: '$Al_xGa_{1-x}As/Al_yGa_{1-y}As$ and GaAs pseudo heterojunction bipolar transistors with lateral emitter resistor', *Appl. Phys. Lett.*, 1993, **62**, pp. 994–996

5 KISHINO, K., ÜNLÜ, M. S., CHYI, J.-I., REED, J., ARSENAULT, L., and MORKOÇ, H.: 'Resonant cavity-enhanced (RCE) photodetectors', *IEEE J. Quantum Electron.*, 1991, **27**, pp. 2025–2034

DIODE-PUMPED SELFSTARTING PASSIVELY MODELOCKED NEODYMIUM-DOPED FIBRE LASER

W. H. Loh, D. Atkinson, P. R. Morkel, R. Grey, A. J. Seeds and D. N. Payne

Indexing terms: Fibre lasers, Lasers

An Nd^{3+}-fibre laser pumped by a single stripe laser diode has been passively modelocked using a semiconductor saturable absorber/end mirror as the mode-locking element. A 6 cm length of heavily doped fibre was used to minimise the effects of positive group velocity dispersion, and stable modelocking with pulses of 4 ps duration was obtained at the laser wavelength of 1053 nm.

Recently, there have been a considerable number of reports on the development of passively modelocked Nd-doped lasers to generate short pulses in the 1 μm wavelength regime [1–7]. A convenient 1 μm short pulse source should be very useful in a large number of applications, such as spectroscopy and the electro-optic sampling of high speed integrated circuits. Both the Nd : YAG and Nd : YLF lasers have been successfully modelocked using some new techniques [3–5]. These lasers, however, have relatively narrow gain bandwidths, which limit the shortest possible pulses to more than 1 ps. This limitation may be circumvented by using disordered crystal [6] or glass fibre hosts. With rare-earth doped bulk crystals, however, relatively high pump powers and low-loss laser cavities are typically required, which limit the use of simple intracavity saturable absorbers. The doped fibre thus has its advantages, as its strong waveguiding nature transforms it into a high gain medium with very low pump power requirements. A passively modelocked Nd-doped fibre laser producing femtosecond pulses has been reported using nonlinear polarisation evolution as the modelocking mechanism [7]. Although this technique is capable of producing very short pulses, it is not easily selfstarting, and the optical powers and fibre lengths required to achieve sufficient nonlinearity to establish modelocking are relatively large. With positive group velocity dispersion inevitable at this wavelength, fibre lengths should ideally be kept as short as possible to reduce the need for dispersion compensation with additional components in the laser cavity. This should not be a problem, however, as heavy Nd^{3+} concentrations, and hence short fibres, are readily achievable without adverse clustering effects.

In this Letter, we demonstrate a passively modelocked Nd-doped fibre laser with a short length of heavily doped fibre and pumped with a single stripe laser diode. The laser is modelocked by an integrated semiconductor intracavity saturable absorber/end mirror which also serves as one end of the laser cavity. A similar integrated semiconductor nonlinear mirror has recently been used to achieve modelocking with an Er^{3+}-doped fibre laser [8], and the current work also serves to demonstrate the general applicability of this simple technique to fibre lasers operating at various wavelengths. The experimental configuration is shown in Fig. 1. The phosphate glass fibre is heavily doped with 1 wt % of Nd^{3+}, and has a length of only 6 cm. It has a spot size of 2·3 μm and an NA of 0·18. It